

ARTICLE

Optimization of Polymer Phase of the Inorganic-Organic Composite Carrier of Extractant Impregnated Adsorbents used in the Extraction Chromatography for MA(III) Separation and Recovery

Tsuyoshi ARAI ^{1*}, Kenta KATSUKI ¹, Hirotsugu ICHIHARA ¹, Yu NAKAMURA ¹,
Hiroki FUKUMOTO ², Yuichi SANO ³, Sou WATANABE ³ and Masayuki TAKEUCHI ³

¹ Shibaura Institute of Technology, 5-3-7, Toyosu, Koto-ku, Tokyo, 135-8548, Japan

² Ibaraki University, 4-12-1, Nakanarusawa-cho, Hitachi-shi, Ibaraki-ken, 316-0033, Japan

³ Japan Atomic Energy Agency, 4-33, Muramatsu, Tokai-mura, Naka-gun, Ibaraki 319-1112, Japan

In this study, we have investigated the optimal structure of the extractant-impregnated adsorbent and the repeatability of the proposed separation flowsheet to establish an efficient MA(III) separation process using extraction chromatography. In the structural optimization of the extractant-impregnated adsorbent, we investigated the adsorption and separation behavior of the adsorbent carrier (SiO₂-P) by varying the styrene divinylbenzene copolymer coating rate from 15% to 0.5%. From these experimental results, it was shown that TEHDGA impregnated adsorbent and HONTA impregnated adsorbent exhibit good adsorption properties even when the Sty-DVB coating rate is reduced to 0.5%. On the other hand, TEHDGA impregnated adsorbent showed good separation behavior even when Sty-DVB coverage was reduced, while tailing was observed in the elution curve for HONTA impregnated adsorbent. From these results, it is suggested that the optimum Sty-DVB coating rate should be determined for each extractant. In this work, we performed a continuous column separation experiment using TEHDGA impregnated adsorbent packed columns with the proposed separation flowsheet. These separation experimental results showed that TEHDGA impregnated adsorbent exhibited good repetitive separation performance, and reproducible chromatograms were obtained. Furthermore, TEHDGA impregnated adsorbent with 0.5% Sty-DVB coating was shown to be a suitable adsorbent for this system with less Ln(III) contamination in the MA intermediate product.

Keywords: minor actinides, extraction chromatography, separation, TEHDGA, HONTA, impregnated adsorbent

I. Introduction

Recovery of trivalent minor actinides (MA(III): Am, Cm) from spent nuclear fuel is an important task for reducing the volume and radiotoxicity of high level radioactive liquid waste.¹⁾ We have developing the extraction chromatography technology to establish more efficient MA(III) recovery processes than solvent extraction processes.²⁻¹⁰⁾ These research results indicated that MA(III) is well separated by extraction chromatography using a combination of N,N,N',N' Tetra (2 Ethylhexyl) Diglycolamide (TEHDGA)¹¹⁾ impregnated adsorbent and N,N,N',N',N"-hexaoctyl nitrilotriacetamide (HONTA)¹²⁾ impregnated adsorbent from high-level radioactive liquid waste. In these studies, we have also investigated the optimization of the extractant impregnation rate, particle size and pore size of the extractant impregnated adsorbent carrier.^{13, 14)} Recently, we have been investigating MA(III) separation from HLLW using the extraction chromatography method by improving the extractant impregnated adsorbent and developing a separation flow sheet for a wide range of spent nuclear fuels.

We focused on optimizing coating rates of the organic phase (styrene-divinylbenzene copolymer : Sty-DVB) on an inorganic-organic composite carrier (SiO₂-P) used in the extractant-impregnated adsorbent. The conventional organic

phase of SiO₂-P has about 15 wt% coating rates, and it has not been studied to optimize the coating rate. If the Sty-DVB coating rate of SiO₂-P could be reduced, it is expected to reduce the load of secondary waste treatment, improve economic efficiency, and reduce radioactive wastes. Therefore, TEHDGA and HONTA impregnated adsorbents were synthesized using SiO₂-P prepared with 0.5 wt% Sty-DVB coating and their adsorption and separation properties were investigated. In these experiments, the effect of the coating rate of Sty-SVB on the adsorption and separation properties for extractant-impregnated adsorbents was evaluated. Moreover, we carried out continuous column separation experiments using the separation flowsheet proposed on the basis of our previous research results, and investigated the effect of Sty-DVB coating rate of the extractant impregnated adsorbent on the separation behaviors.

II. Experimental

1. Preparation of Extractant Impregnated Adsorbents

The extractant impregnated adsorbent was obtained by impregnating 20 wt% each of TEHDGA and HONTA extractants on SiO₂-P coated with 0.5 wt% of Sty-DVB (cross-linking ratio : 15%) on porous SiO₂ particles. In this work, conventional extractant impregnated adsorbent (Sty-DVB coating rate : 15 wt%, extractant impregnation rate : 20 wt%) was also used as a comparison material. Detail

*Corresponding author, E-mail: t-arai@shibaura-it.ac.jp

procedure can be found in the reference.¹⁵⁾ In this paper, the adsorbent with 0.5 wt% coverage is referred to as L-type (L-TEHDGA, L-HONTA) and the conventional adsorbent with 15 wt% coverage as E-Type (E-TEHDGA, E-HONTA). **Figure 1** shows structures of TEHDGA and HONTA extractant, and **Table 1** shows characteristics of E-type and L-type adsorbents.

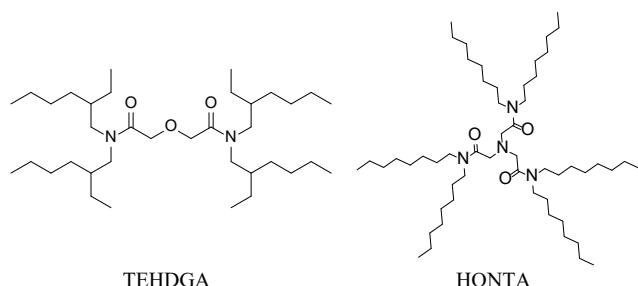


Fig. 1 Structure of TEHDGA and HONTA extractant

Table 1 Characteristics of E-type and L-type adsorbents

Adsorbent	E-type	L-type
Particle diameter [μm]	50	100
Sty-DVB cross-linking rate [%]	15	15
Sty-DVB coating rate [wt%]	15	0.5
Impregnation rate [wt%]	20	20
Surface area [cm^2/g]	47.2	7.8
Pore volume [cm^3/g]	2.5×10^{-2}	4.1×10^{-3}

2. Evaluation of the Effect of Sty-DVB Coating Rate on Adsorption Performance

In order to evaluate the effect of structural changes in $\text{SiO}_2\text{-P}$ carriers on adsorption performance, batch adsorption experiments were conducted. **Table 2** shows conditions for batch adsorption experiments. In the batch adsorption experiments, each adsorbent and the test solution were placed in a test tube and shaken based on this table. The test solutions were prepared using a nitric acid solution at the specified concentration to obtain 10 mM of Nd(III).

Table 2 Conditions for batch adsorption experiments

Condition item	Setting conditions	
Adsorbent	TEHDGA	HONTA
Nd(III) conc. [mM]	10	
HNO_3 conc. [M]	$10^{-2} - 10$	$10^{-3} - 1$
Ads. : Sol. [g : cm^3]	1 : 20	
Contact time [min]	60	
Shaking rate [$\text{rev} \cdot \text{min}^{-1}$]	160	
Shaking width [mm]	40	
Temperature [$^{\circ}\text{C}$]	25	

The concentration of Nd(III) in the aqueous phase before and after the batch adsorption experiments was measured by ICP-OES. Adsorption performance was evaluated by distribution coefficient K_d expressed by Ref. (1).

$$K_d = \frac{(C_{\text{aq. ctrl}} - C_{\text{aq.}})}{C_{\text{aq.}}} \times \frac{V}{W_R} \quad (1)$$

where, $C_{\text{aq. ctrl}}$ is the metal concentration in the initial solution [mM], $C_{\text{aq.}}$ is the metal concentration after adsorption [mM],

V is the volume of the test solution [cm^3], and W_R is the dry weight of the adsorbent [g].

3. Evaluation of the Effect of Sty-DVB Coating Rate on Separation Performance

In this work, column separation experiments were conducted to evaluate the effect of Sty-DVB coating rate of the extractant impregnated adsorbent on separation performance. **Figure 2** shows schematic diagram of the column experiment apparatus. For the column separation experiments, glass columns of $\phi 10 \text{ mm} \times h 200 \text{ mm}$ were packed with each of the E-type and L-type impregnated adsorbents to a packing height of 150 mm.

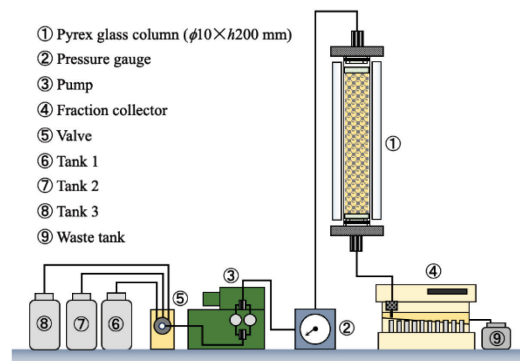


Fig. 2 Schematic diagram of the column experiment apparatus

(1) Investigation of the Separation Behavior of TEHDGA Adsorbent

Table 3 shows conditions for TEHDGA adsorbent column experiments, and **Table 4** shows metal ion concentration in the simulated HLLW. Also, the nitric acid concentration of the simulated HLLW was adjusted to 2.8 M.

Table 3 Conditions for TEHDGA adsorbent column experiments

Condition item		Setting conditions
Column [mm]		$\phi 10 \times h 200$
Filling height [mm]		150
Filling volume [cm^3]		11.8
Flow procedure (Volume [cm^3])	1 Test solution (24)	Simulated HLLW
	2 Washing solution (72)	7 M HNO_3
	3 Eluent (60)	Distilled water
Flow Rate [$\text{cm}^3 \cdot \text{min}^{-1}$]		3
Temperature [$^{\circ}\text{C}$]		50

Table 4 Metal ion concentration in simulated HLLW

Metal ion	Conc. [mM]	Metal ion	Conc. [mM]
Cr(III)	0.09	Sn(IV)	0.23
Mn(II)	2.50	Sb(III)	1.92
Fe(III)	1.78	Ba(II)	2.98
Ni(II)	0.19	La(III)	1.80
Sr(II)	0.56	Ce(III)	2.02
Y(III)	0.34	Pr(III)	1.05
Zr(IV)	4.04	Nd(III)	3.52
Mo(VI)	4.50	Sm(III)	0.87
Ru(III)	4.78	Eu(III)	0.15
Rh(III)	1.21	Gd(III)	6.96
Pd(II)	3.30		

In the column separation experiments for TEHDGA adsorbent, the simulated HLLW, washing solution and eluent were passed through the column, which was kept at 50°C, using a double plunger pump at a flow rate of 3 cm³·min⁻¹, and the liquid flowing out of the bottom of the column was collected in 3 cm³ fractions using a fraction collector. The metal ion concentration in each fraction was measured by ICP-OES.

(2) Investigation of the Separation Behavior of HONTA Adsorbent

Table 5 shows conditions for HONTA adsorbent column experiments, and **Table 6** shows metal ion concentration in the simulated MA(III) intermediate product. Also, the nitric acid concentration of the MA(III) intermediate product was adjusted to 0.2 M. In the column separation experiments for HONTA adsorbent, the simulated MA(III) intermediate product, washing solution and eluent were passed through the column, which was kept at 25°C, using a double plunger pump at a flow rate of 1 cm³·min⁻¹, and the liquid flowing out of the bottom of the column was collected in 3 cm³ fractions using a fraction collector. In this experiment, fractions collected from L-TEHDGA adsorbent column experiment eluent were used as the simulated MA(III) intermediate product.

Table 5 Conditions for HONTA adsorbent column experiments

Condition item		Setting conditions
Column [mm]		φ 10 × h 200
Filling height [mm]		150
Filling volume [cm ³]		11.8
Flow procedure (Volume [cm ³])	1 Test solution (12)	Simulated MA(III) intermediate product
	2 Washing solution (36)	0.2 M HNO ₃
	3 Eluent (30)	1 M HNO ₃
Flow Rate [cm ³ ·min ⁻¹]		1
Temperature [°C]		25

Table 6 Metal ion concentration in simulated MA(III) intermediate product

Metal ion	Conc. [mM]	Metal ion	Conc. [mM]
Y(III)	0.09	Pr(III)	4.50
Zr(IV)	2.50	Nd(III)	4.78
Mo(VI)	1.78	Sm(III)	1.21
Sb(III)	0.19	Eu(III)	3.30
La(III)	0.56	Gd(III)	0.23
Ce(III)	0.34		

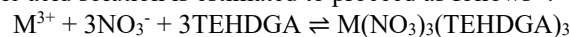
(3) Investigation of Adsorption-elution Stability of L-TEHDGA Adsorbent

In this study, we conducted repeatedly column experiments to examine adsorption-elution stability of L-TEHDGA adsorbent with changes in Sty-DVB coating rate. In this experiment, column experiments were conducted 10 cycles using L-TEHDGA adsorbent packed column based on the conditions in Table 3, and the stability of TEHDGA adsorbent was evaluated based on the chromatograms and recovery rates of metal ions for each cycle.

III. Results and Discussion

1. Evaluation of the Effect of Sty-DVB Coating Rate on Adsorption Performance

In order to investigate the effect of Sty-DVB coating rate on the adsorption behavior of the extractant-impregnated adsorbent, batch adsorption experiments were conducted for Nd(III). **Figure 3** shows dependence of Nd(III) distribution coefficients on nitric acid concentration for E-TEHDGA and L-TEHDGA adsorbent. In this experiment, the distribution coefficient was calculated from the average of two experiments. As shown in Fig. 3, the distribution coefficient increased with the increase in nitric acid concentration for each TEHDGA adsorbent. TEHDGA is a neutral molecule, and the reaction for extracting trivalent metal ions from a nitric acid solution is estimated to proceed as follows²⁾:



In addition, it was confirmed that the distribution coefficient of L-TEHDGA decreased more than that of E-TEHDGA at 10 M nitric acid concentration. Therefore, TEHDGA adsorbent has good adsorption performance for Nd(III) even when Sty-DVB coating rate is reduced to 0.5%.

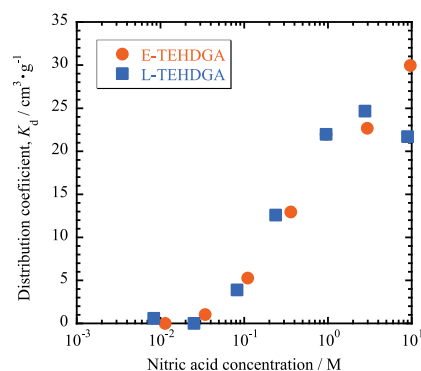


Fig. 3 Dependence of Nd(III) distribution coefficients on nitric acid concentration for TEHDGA adsorbents

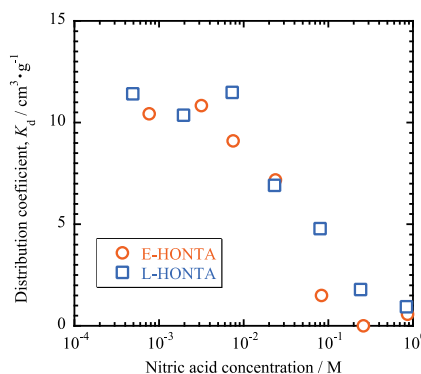


Fig. 4 Dependence of Nd(III) distribution coefficients on nitric acid concentration for HONTA adsorbents

Figure 4 shows dependence of Nd(III) distribution coefficients on nitric acid concentration for E-HONTA and L-HONTA adsorbent. From Fig. 4, HONTA adsorbent showed similar adsorption behavior on any of the carriers, and the adsorption distribution coefficient decreased with increasing nitric acid concentration. However, in this experiment, HONTA extractant detached from L-HONTA adsorbent was observed on surface of aqueous phase in a high concentration

of nitric acid. On the other hand, detachment of HONTA extractant from E-HONTA was not observed. It was suggested that there was a concern that HONTA extractant might detach from HONTA adsorbent when the coating rate of Sty-DVB decreased.

From these results, it was considered that the coating rate of Sty-DVB on SiO₂-P should be optimized depending on extractant types.

2. Investigation of the Separation Behavior of TEHDGA Adsorbent

Figure 5 shows the results of a separation experiment for simulated HLLW using E-TEHDGA adsorbent packed column. Table 7 shows recovery rate for each metal ion using E-TEHDGA adsorbent, and the recovery rate in “D” section, which is MA(III) intermediate product in brackets.

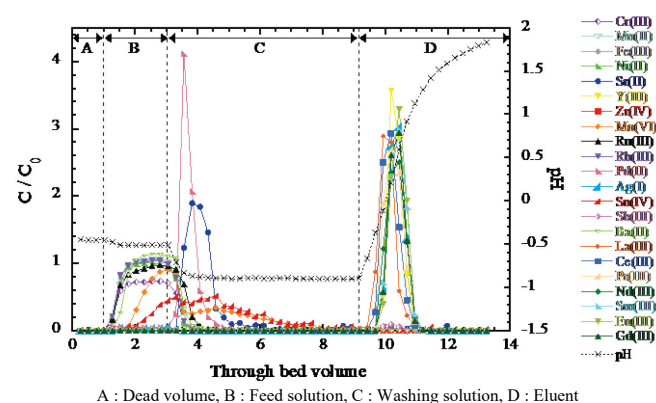


Fig. 5 Results of separation experiments using E-TEHDGA adsorbent column

Table 7 Recovery rate for each metal ion using E-TEHDGA adsorbent (recovery rate of “D” section in brackets)

Metal ion	Recovery [%]	Metal ion	Recovery [%]
Cr(III)	72.0 (0)	Sn(IV)	88.6 (1.33)
Mn(II)	100 (0)	Sb(III)	5.6 (3.1)
Fe(III)	99.6 (0)	Ba(II)	100 (0.01)
Ni(II)	97.7 (0.71)	La(III)	97.1 (93.9)
Sr(II)	96.9 (1.92)	Ce(III)	97.4 (97.4)
Y(III)	97.3 (97.3)	Pr(III)	100 (100)
Zr(IV)	1.1 (0.72)	Nd(III)	94.7 (94.7)
Mo(VI)	98.8 (0.76)	Sm(III)	100 (100)
Ru(III)	100 (0.12)	Eu(III)	100 (100)
Rh(III)	100 (0.44)	Gd(III)	95.3 (95.3)
Pd(II)	98.5 (0)		

As shown Fig. 5, the elution peaks of Sr(II) and Pd(II) were detected after passing through the washing solution, and the sharp elution peak of Ln(III) was detected after passing through the eluent. Therefore, it was confirmed that the simulated HLLW was successfully partitioned into Ln(III) group and other FPs using E-TEHDGA packed column. It is assumed that MA(III) will be eluted with Ln(III) in “D” section in the eluent, and this recovered solution will be MA(III) intermediate product.

On the other hand, it was found that Zr(IV) and Sb(III) were not eluted and accumulated into E-TEHDGA adsorbent. However, it has been confirmed that Zr(IV) and Sb(III) are

able to be eluted using EDTA solution, so it is expected that this will not influence repeatedly use of the column.

Figure 6 shows the results of a separation experiment for simulated HLLW using L-TEHDGA adsorbent packed column. Table 8 shows recovery rate for each metal ion using L-TEHDGA adsorbent, and the recovery rate in “D” section.

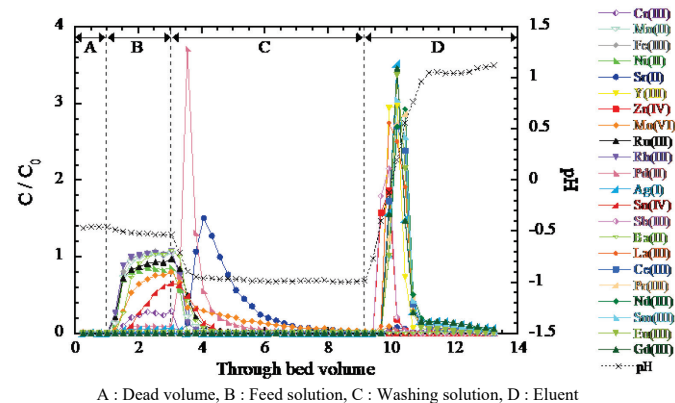


Fig. 6 Results of separation experiments using L-TEHDGA adsorbent column

Table 8 Recovery rate for each metal ion using L-TEHDGA adsorbent (recovery rate of “D” section in brackets)

Metal ion	Recovery [%]	Metal ion	Recovery [%]
Cr(III)	20.0 (0)	Sn(IV)	53.1 (0)
Mn(II)	99.7 (0)	Sb(III)	52.3 (52.2)
Fe(III)	100 (0)	Ba(II)	96.96 (0)
Ni(II)	79.5 (0)	La(III)	100 (100)
Sr(II)	100 (2.14)	Ce(III)	96.7 (96.7)
Y(III)	85.0 (85.0)	Pr(III)	100 (100)
Zr(IV)	45.8 (45.6)	Nd(III)	100 (100)
Mo(VI)	100 (3)	Sm(III)	100 (100)
Ru(III)	100 (0)	Eu(III)	87.9 (87.9)
Rh(III)	100 (0)	Gd(III)	99.5 (99.5)
Pd(II)	100 (1.41)		

From this experimental result, it was shown that the simulated HLLW was successfully partitioned into Ln(III) group and other FPs using the L-TEHDGA packed column in the same way as E-TEHDGA packed column. On the other hand, it was observed that L-TEHDGA had longer tailing of Sr(II) than E-TEHDGA. In addition, Zr(IV) and Sb(III) showed elution peaks after the eluent had passed through, and they were contaminated in MA(III) intermediate product. These results are considered to be due to low Sty-DVB coating rate of L-TEHDGA, which caused the extractant to be impregnated in multiple layers locally, and it took time for the solution to diffuse.

3. Investigation of the Separation Behavior of HONTA Adsorbent

In this work, we conducted separation experiments using HONTA-packed column for “D” section solutions collected in L-TEHDGA column experiment (Fig. 6).

Figure 7 shows separation results for simulated MA(III) intermediate products using E-HONTA adsorbent packed column. Table 9 shows recovery rate for each metal ion using

E-HONTA adsorbent, and the recovery rate in “D” section, which is MA(III) product in brackets. We expect that MA(III) will be eluted in section “D” where the eluent is passed through the column.

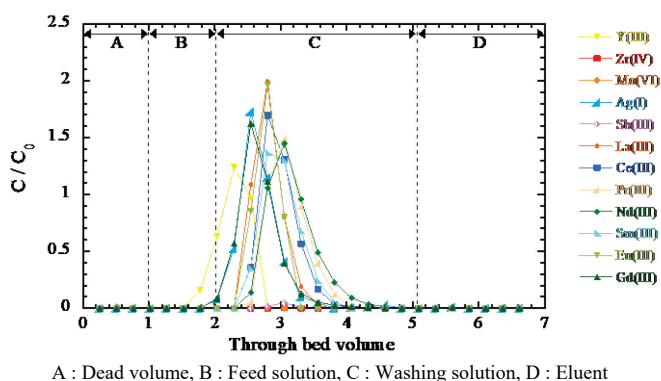


Fig. 7 Results of separation experiments using E-HONTA adsorbent column

Table 9 Recovery rate for each metal ion using E-HONTA adsorbent (recovery rate of “D” section in brackets)

Metal ion	Recovery [%]	Metal ion	Recovery [%]
Y(III)	75.11 (0)	Pr(III)	100 (0)
Zr(IV)	0.12 (0)	Nd(III)	100 (0)
Mo(VI)	0 (0)	Sm(III)	99.98 (0)
Sb(III)	2.03 (0)	Eu(III)	90.52 (0)
La(III)	100 (0)	Gd(III)	100 (0.2)
Ce(III)	100 (0)		

From Fig. 7, it was confirmed that the elution peak of Y(III) and Ln(III) appeared after the washing solution was passed through the column. This result indicated the possibility of MA(III) and Ln(III) separation. On the other hand, it was found that Zr(IV), Mo(VI) and Sb(III) were hardly eluted and accumulated into E-HONTA adsorbent. For this reason, it is necessary to remove these elements from MA(III) intermediate product in advance, or to recover them after passing through the eluent.

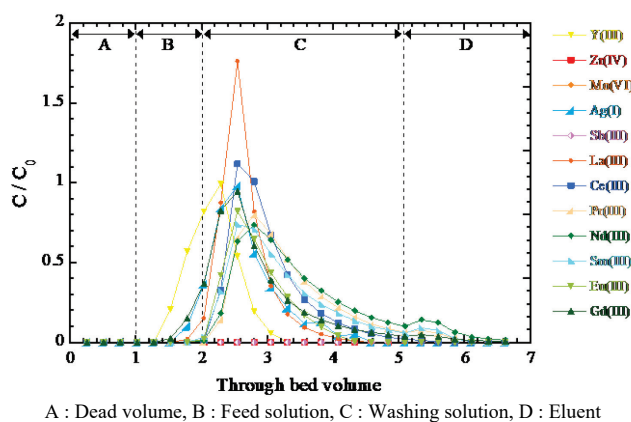


Fig. 8 Results of separation experiments using L-HONTA adsorbent column

Figure 8 shows separation results for simulated MA(III) intermediate products using L-HONTA adsorbent packed column. **Table 10** shows recovery rate for each metal ion

using L-HONTA adsorbent, and the recovery rate in “D” section. From Fig. 8, elution curves of Y(III) and Ln(III) by L-HONTA adsorbent packed column showed longer tailing than E-HONTA adsorbent. This is expected to improve due to a reduction in flow rate, but it might also cause a decrease in separation efficiency. In addition, it was confirmed that part of Ln(III) was contaminated into MA(III) products.

From these results, it was considered that the separation behavior of HONTA adsorbent is affected by Sty-DVB coating rate.

Table 10 Recovery rate for each metal ion using L-HONTA adsorbent (recovery rate of “D” section in brackets)

Metal ion	Recovery [%]	Metal ion	Recovery [%]
Y(III)	84.29 (0)	Pr(III)	100 (3.92)
Zr(IV)	0 (0)	Nd(III)	100 (9.86)
Mo(VI)	0 (0)	Sm(III)	100 (4.74)
Sb(III)	0 (0)	Eu(III)	73.38 (0)
La(III)	100 (0)	Gd(III)	100 (3.2)
Ce(III)	100 (0.38)		

4. Investigation of Adsorption-elution Stability of L-TEHDGA Adsorbent

In this study, we tried to evaluate adsorption-elution stability of L-TEHDGA adsorbent with repeated column separation experiments. **Figure 9** shows separation experiment results of simulated HLLW repeatedly using L-TEHDGA packed columns (1st, 5th and 10th cycles). **Table 11** shows recovery rates of metal ions in each cycle using L-TEHDGA adsorbent, and the recovery rate in “D” section.

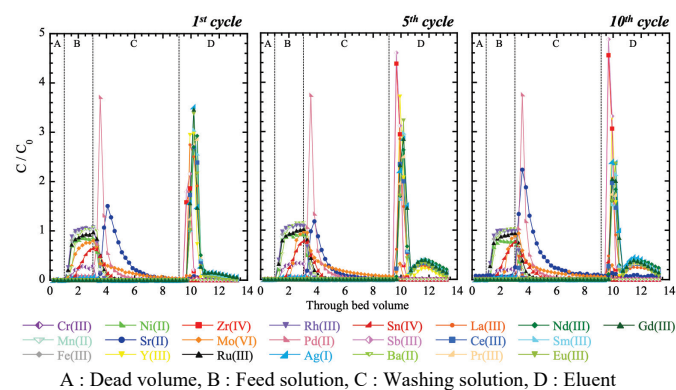


Fig. 9 Separation experiment results of simulated HLLW repeatedly using L-TEHDGA adsorbent packed columns

From Fig. 9, it was indicated that Sr(II) elution peak has tailing, and there was a difference depending on the cycle. The elution peaks of Zr(IV) and Sb(III) appeared immediately after the eluent was passed through the column, and the elution peak of Ln(III) appeared after a slight delay. In addition, the recovery rate of Ln(III) in the MA(III) intermediate product was almost 100% for all Ln(III) up to the 5th cycle, but in the 10th cycle, La(III) was approximately 73% and other Ln(III) was approximately 85%. From these experimental results, the chromatograms for each cycle showed good reproducibility, and it was indicated that the L-TEHDGA adsorbent is reusable. However, there was concern

that Zr(IV) and Sb(III) might be mixed into the MA(III) intermediate product in the 1st cycle, and it is necessary to investigate methods for removing Zr(IV) and Sb(III) in the future. In addition, since the overall recovery rate is approximately 90 %, it is necessary to further improve the adsorbent and examine the elution conditions in detail.

Table 11 Recovery rates of metal ions in each cycle using L-TEHDGA adsorbent (recovery rate of “D” section in brackets)

Metal ion	1st	5th	10th	overall
Cr(III)	20.0 (0)	25.4 (0)	15.5 (0)	17.9
Mn(II)	99.7 (0)	100 (0)	95.7 (0)	99.4
Fe(III)	100 (0)	100 (0)	96.5 (0)	100
Ni(II)	79.5 (0)	86.3 (0)	71.7 (0)	78.1
Sr(II)	100 (2.1)	68.0 (0.4)	100 (15.6)	99.8
Y(III)	85.0 (85.0)	89.6 (89.6)	88.7 (88.7)	81.4
Zr(IV)	45.8 (45.6)	95.6 (95.6)	98.0 (98.0)	92.1
Mo(VI)	100 (3)	100 (8.24)	99.7 (6.75)	100
Ru(III)	100 (0)	100 (0)	99 (0)	100
Rh(III)	100 (0)	100 (0)	98.4 (0)	100
Pd(II)	100 (1.41)	100 (1.45)	100 (1.07)	100
Ag(I)	100 (100)	100 (100)	100 (100)	100
Sn(IV)	53.1 (0)	59.5 (0)	68.8 (4.7)	53.6
Sb(III)	52.3 (52.3)	100 (100)	100 (100)	99.9
Ba(II)	97.0 (0)	100 (0.05)	94.8 (0.08)	98.3
La(III)	100 (100)	99.9 (98.4)	85.9 (72.9)	90.8
Ce(III)	96.7 (96.7)	99.0 (99.0)	88.8 (85.2)	89.3
Pr(III)	100 (100)	100 (100)	87.0 (86.2)	91.9
Nd(III)	100 (100)	100 (100)	90.4 (90.2)	94.3
Sm(III)	100 (100)	100 (100)	89.6 (89.6)	94.5
Eu(III)	87.9 (87.9)	93.7 (93.7)	81.1 (81.1)	82.6
Gd(III)	99.5 (99.5)	100 (100)	99.8 (99.8)	98.4

IV. Conclusion

In this work, TEHDGA and HONTA adsorbents were synthesized using SiO₂-P prepared with Sty-DVB at coating rates of 0.5 wt%, and their adsorption characteristics and separation performance were evaluated. It was considered that TEHDGA adsorbent has good adsorption performance for Nd(III) even when Sty-DVB coating rate is reduced to 0.5 wt%. In addition, it was confirmed that L-TEHDGA adsorbent exhibits separation behavior similar to that of E-TEHDGA adsorbent. On the other hand, it was found that separation behavior of HONTA adsorbent is affected by Sty-DVB coating rate. Moreover, chromatograms for each cycle showed good reproducibility, and overall recovery rate was generally 90 % or more, which showed that L-TEHDGA adsorbent is reusable and has stable adsorption-elution performance.

Acknowledgment

This work was carried out as a part of the research project "Basic Research Programs of Vitrification Technology for Waste Volume Reduction (JPJ010599)", commissioned by the Ministry of Economy, Trade and Industry (METI), in FY2019 – 2023.

References

- 1) International Atomic Energy Agency (2004) Technical Reports Series No. 435; Implications of Partitioning and Transmutation in Radioactive Waste Management. IAEA, Vienna
- 2) Y. Horiuchi, S. Watanabe, Y. Sano, M. Takeuchi, F. Kida, T. Arai, "Development of MA separation process with TEHDGA/SiO₂-P for an advanced reprocessing," *J. Radioanal. Nucl. Chem.*, **330**, 237-244 (2021).
- 3) S. Watanabe, T. Senzaki, A. Shibata, K. Nomura, M. Takeuchi, K. Nakatani, H. Matsuura, Y. Horiuchi, T. Arai, "Improvement in flow-sheet of extraction chromatography for trivalent minor actinides recovery," *J. Radioanal. Nucl. Chem.*, **322**, 1273-1277 (2019).
- 4) M. Takeuchi, S. Watanabe, Y. Sano, H. Kofuji, H. Suzuki, T. Matsumura, "Characterization of HONTA/SiO₂-P adsorbent for MA(III)/Ln(III) separation flow-sheet," *Proc. Int. Conf. on Global 2019*, Seattle, WA, USA, Sept. 22-27, 2019, 783-788 (2019).
- 5) S. Watanabe, Y. Sano, H. Kofuji, M. Takeuchi, A. Shibata, K. Nomura, "Am, Cm recovery from genuine HLLW by extraction chromatography," *J. Radioanal. Nucl. Chem.*, **316**, 1113-1117 (2018).
- 6) S. Watanabe, K. Nomura, S. Kitawaki, A. Shibata, H. Kofuji, Y. Sano, M. Takeuchi, "Flow-sheet study of MA recovery by extraction chromatography for SmART cycle project," *Procedia Chemistry*, **21**, 101-108 (2016).
- 7) S. Watanabe, Y. Sano, K. Nomura, Y. Koma, Y. Okamoto, "Safety operation of chromatography column system with discharging hydrogen radiolytically generated," *EPJ Nuclear Sci. Technol.*, **1**, 9 (2015).
- 8) S. Watanabe, I. Goto, K. Nomura, Y. Sano, Y. Koma, "Extraction Chromatography Experiments on Repeated Operation using Engineering Scale Column System," *Energy Procedia*, **7**, 449-453 (2011).
- 9) S. Watanabe, I. Goto, Y. Sano, Y. Koma, "Chromatography Column System with Controlled Flow and Temperature for Engineering Scale Application," *J. Eng. Gas Turbines Power*, **132**[10], 102903 (2010)
- 10) T. Akuzawa, S. Kim, M. Kubota, H. Wu, S. Watanabe, Y. Sano, M. Takeuchi, T. Arai, "Design of MA(III)/Ln(III) separation process of extraction chromatography technology," *J. Radioanal. Nucl. Chem.*, **331**, 5851-5858 (2022).
- 11) P. Deepika, K. N. Sabharwal, T. G. Srinivasan, P. R. Vasudeva Rao, "Studies on the Use of N,N,N',N'-Tetra(2-ethylhexyl) Diglycolamide (TEHDGA) for Actinide Partitioning. I : Investigation on Third-Phase Formation and Extraction Behavior," *Solvent Extr. Ion Exch.*, **28**[2], 184-201 (2010).
- 12) Y. Sasaki, Y. Tsubata, Y. Kitatsuji, Y. Morita, "Novel Soft-Hard Donor Ligand, NTAamide, for Mutual Separation of Trivalent Actinoids and Lanthanoids," *Chem. Lett.*, **42**[1], 91-92 (2013).
- 13) S. Watanabe, Y. Sano, S. Sanda, S. Sakurai, T. Arai, "Influences of Pore and Particle Sizes of CMPO/SiO₂-P Adsorbent on Extraction Chromatography Process," *J. Ion Exchange*, **30**[1], 8-16 (2019).
- 14) S. Watanabe, T. Arai, T. Ogawa, M. Takizawa, K. Sano, K. Nomura, Y. Koma, "Optimizing composition of TODGA/SiO₂-P adsorbent for extraction chromatography process," *Procedia Chemistry*, **7**, 411-417 (2012).
- 15) Y. Wei, M. Kumagai, Y. Takashima, G. Modolo, R. Odoj, "Studies on the separation of minor actinides from high-level wastes by extraction chromatography using novel silica-based extraction resins," *Nucl. Technol.*, **132**[3], 413-423 (20)